Synthesis and crystal structure of the conjugated tetrayne $(\eta^5\text{-}C_5Me_5)Re(NO)(PPh_3)(C{\equiv}CC{\equiv}CC{\equiv}CC{\equiv}CSiMe_3)$: application of the Cadiot-Chodkiewicz coupling reaction to the chain extension of metal-capped *sp*-carbon wires

Berit BARTIK, Roman DEMBINSKI, Tamás BARTIK, Atta M. ARIF and J. A. GLADYSZ*

Department of Chemistry, University of Utah, Salt Lake City, UT 84112, USA.

Received July 1, 1996; accepted November 18, 1996.

Abstract. – Sequential reactions of the butadiynyl complex $(\eta^5\text{-}C_5Me_5)Re(NO)(PPh_3)(C{\equiv}CC{\equiv}CH)$ with *n*-BuLi, CuI, and $Me_3SiC{\equiv}CC{\equiv}CBr$ (THF/$EtNH_2$, −45 to −20 °C) give the 1,3,5,7-tetrayne $(\eta^5\text{-}C_5Me_5)Re(NO)(PPh_3)(C{\equiv}CC{\equiv}CC{\equiv}CC{\equiv}CSiMe_3)$ (**8**) in 77% yield. This involves an intermediate $ReC{\equiv}CC{\equiv}CCu$ species, and constitutes one of the first examples of a Cadiot-Chodkiewicz coupling in a metal coordination sphere. The crystal structure of **8** (monoclinic, $P2_1/n$ (No. 14), $a = 16.685(5)$ Å, $b = 13.211(2)$ Å, $c = 18.067(4)$ Å, $\beta = 109.97(2)°$, $Z = 4$) is analyzed in detail. The eight bond angles associated with the $ReC{\equiv}CC{\equiv}CC{\equiv}CC{\equiv}CSi$ unit range from 175.9(8)° to 179(1)°. Other reactions that have been used to construct polyalkynyl *sp*-carbon chains, in which at least one of the two endgroups is the chiral rhenium fragment $(\eta^5\text{-}C_5Me_5)Re(NO)(PPh_3)$, are discussed.

Key words : bromodiyne, butadiynyl complexes, rhenium, 1,3,5,7-tetrayne crystal structure.

Résumé. – Synthèse et structure cristalline du complexe $(\eta^5\text{-}C_5Me_5)Re(NO)(PPh_3)(C{\equiv}CC{\equiv}CC{\equiv}CC{\equiv}CSiMe_3)$ à chaîne tetrayne conjuguée : application de la réaction de couplage Cadiot-Chodkiewicz à l'allongement de chaînes d'atomes de carbones hybrides *sp* pontant deux greffons organométalliques $(\eta^5\text{-}C_5Me_5)Re(NO)(PPh_3)$. Les réactions séquentielles du complexe butadiynyle $(\eta^5\text{-}C_5Me_5)Re(NO)(PPh_3)(C{\equiv}CC{\equiv}CH)$ avec *n*-BuLi, CuI et $Me_3SiC{\equiv}CC{\equiv}CBr$ (THF/$EtNH_2$, de −45 à −20 °C) conduisent au complexe $(\eta^5\text{-}C_5Me_5)Re(NO)(PPh_3)(C{\equiv}CC{\equiv}CC{\equiv}CC{\equiv}CSiMe_3)$ (**8**) à chaîne 1,3,5,7-tétrayne conjuguée, avec un rendement de 77%. L'obtention du complexe **8** implique une espèce intermédiaire $ReC{\equiv}CC{\equiv}CCu$ et constitue l'un des premiers exemples d'un couplage Cadiot-Chodkiewicz dans la sphère de coordination d'un métal. La structure cristalline du complexe **8** (monoclinique, $P2_1/n$ (No. 14), $a = 16{,}685(5)$ Å, $b = 13{,}211(2)$ Å, $c = 18{,}067(4)$ Å, $\beta = 109{,}97(2)°$, $Z = 4$) est analysée en détail. Les huit angles de liaison associés à l'unité $ReC{\equiv}CC{\equiv}CC{\equiv}CC{\equiv}CSi$ varient de 175,9(8)° à 179(1)°. Les autres réactions utilisées pour l'élaboration des chaînes polyalkynyle d'atomes de carbone hybrides *sp*, dont au moins une des extrémités est le greffon chiral $(\eta^5\text{-}C_5Me_5)Re(NO)(PPh_3)$, sont discutées.

Introduction

There is currently intense interest in compounds in which elemental *sp*-carbon chains span two transition metals [1]. Among many possible fundamental and applied attributes, complexes with very long, wire-like chains [2] may serve as models for the one-dimensional polymeric carbon allotrope, which is often termed "carbyne" [3]. Although syntheses of "carbyne" have been reported, the material remains less than completely characterized, especially by comparison to the familiar two-dimensional sp^2- and three-dimensional sp^3 polymeric carbon allotropes, graphite and diamond [4].

To date, all synthetic approaches to "carbyne", or models thereof, yield a distribution of molecular weights. However, we have sought to develop methodologies that will give metal-capped species of homogeneous chain lengths. In this paper, which is based upon a lecture given at the "13th Summer School in Coordination Chemistry" (Polanica-Zdrój, Poland, June 1996), we first briefly review and analyze synthetic strategies for polyalkynyl or $(C{\equiv}C)_n$ compounds in which at least one endgroup is the chiral rhenium fragment $(\eta^5\text{-}C_5Me_5)Re(NO)(PPh_3)$ (**I**) [5-7]. We then report a heretofore unpublished experimental procedure for a key step, a Cadiot-Chodkiewicz coupling. Finally, we describe the

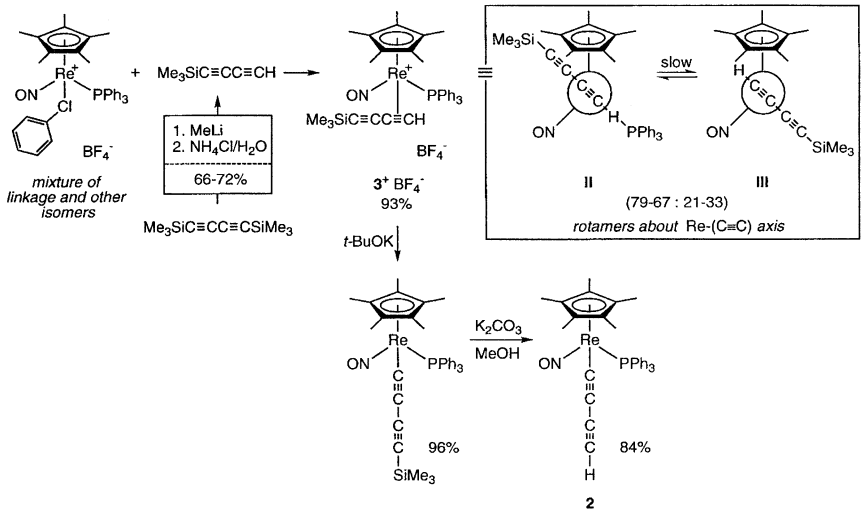

Scheme 1. – Synthesis of a rhenium butadiynyl complex.

crystal structure of the coupling product, a 1,3,5,7-octatetrayne. Metrical parameters associated with the *sp*-carbon chain and packing mode are analyzed in detail, and compared with those of other structurally characterized tetraynes.

Review of methodology

Many protocols have been developed for the oxidative coupling of terminal alkynes to 1,3-diynes [8, 9]. Furthermore, ethynyl and 1,3-butadiynyl complexes of the rhenium fragment **I**, $(\eta^5\text{-}C_5Me_5)Re(NO)(PPh_3)(C{\equiv}CH)$ (**1**) and $(\eta^5\text{-}C_5Me_5)Re(NO)(PPh_3)(C{\equiv}CC{\equiv}CH)$ (**2**), are readily available [6a]. For example, the latter can be prepared as outlined in Scheme 1. The key *sp*-carbon building block, $Me_3SiC{\equiv}CC{\equiv}CH$, can be accessed in good yield by the reaction of $Me_3SiC{\equiv}CC{\equiv}CSiMe_3$ with MeLi to give $Me_3SiC{\equiv}CC{\equiv}CLi$ and Me_4Si, followed by the addition of aqueous NH_4Cl [10]. The intermediate cationic π-alkyne complex $\mathbf{3}^+BF_4^-$ is obtained as a mixture of isomers (**II**, **III**) that differ by a ca. 180° rotation about the Re–(C≡C) axis, and do not interconvert on the NMR timescale at room temperature.

The Eglinton oxidative-coupling procedure utilizes a stoichiometric amount of Cu(II) [9] and efficiently transforms both **1** and **2** to the corresponding dirhenium μ-polyynediyl complexes. For example, as shown in Scheme 2, the reaction of **2** with $Cu(OAc)_2$ (1.5 equiv) in pyridine at 80 °C gives the μ-octatetraynediyl complex $(\eta^5\text{-}C_5Me_5)Re(NO)(PPh_3)$-$(C{\equiv}CC{\equiv}CC{\equiv}CC{\equiv}C)(Ph_3P)(ON)Re(\eta^5\text{-}C_5Me_5)$ (**4**) in 70% yield [5c]. In all cases, the dirhenium products are obtained as ca. 50:50 mixtures of *meso* and *dl* diastereomers.

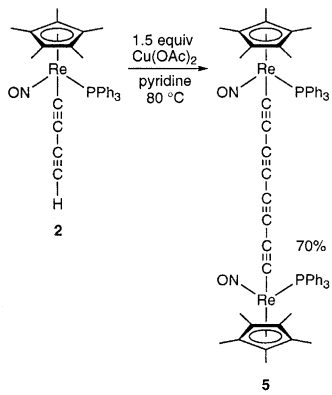

Scheme 2. – Synthesis of a dirhenium μ-octatetraynediyl complex by an Eglinton coupling reaction.

No upper limit has been established for the chain length of the polyalkynyl substrate in the Eglinton coupling [9]. Indeed, Scheme 2 has been extended to the synthesis of dirhenium complexes with C_{20} or μ-icosadecaynediyl chains [5d]. Thus, the key issue becomes the preparation of higher homologs of **1** and **2**, $(\eta^5\text{-}C_5Me_5)Re(NO)(PPh_3)((C{\equiv}C)_nH)$. Towards this end, either (1) organic building blocks with longer *sp*-carbon chains or (2) additional types of coupling reactions that can operate within the coordination sphere of the rhenium fragment **I** are required. Importantly, 1,3,5,7-tetraynes that bear one silyl and one hydrogen endgroup are much less stable than $Me_3SiC{\equiv}CC{\equiv}CH$ and only a few have been described in the literature [11]. Therefore, polyalkynyl building blocks with *two* silyl endgroups were investigated first.

Accordingly, the known and robust di(silyl) 1,3,5,7-tetrayne $Me_3SiC{\equiv}CC{\equiv}CC{\equiv}CC{\equiv}CSiMe_3$ can be

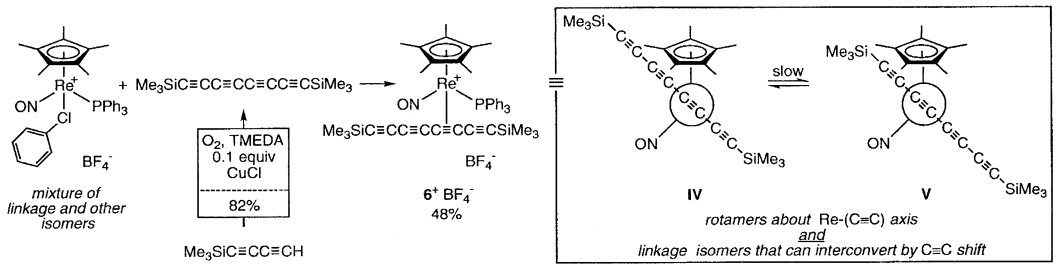

Scheme 3. – Synthesis of a rhenium π-octatetrayne complex.

prepared from $Me_3SiC{\equiv}CC{\equiv}CH$ by the Glaser oxidative coupling shown in Scheme 3 [6a, 12]. This protocol, which uses a catalytic amount of Cu(I) and a stoichiometric amount of O_2, is much less effective with the rhenium substrates **1** and **2**. Application of the substitution procedure in Scheme 1 gives the cationic π-alkyne complex $[(\eta^5\text{-}C_5Me_5)Re(NO)(PPh_3)(Me_3SiC{\equiv}CC{\equiv}CC{\equiv}CC{\equiv}CSiMe_3)]^+BF_4^-$ (**6**$^+BF_4^-$), in which the rhenium is bound to the internal C≡C moieties. As with **3**$^+BF_4^-$ in Scheme 1, **6**$^+BF_4^-$ is a mixture of two isomers (60:40) that differ by a 180° rotation about the Re–(C≡C) axis (**IV** and **V**) and do not interconvert on the NMR timescale at room temperature. With **6**$^+BF_4^-$, these also constitute *linkage* isomers that could interconvert by a shift of rhenium from one internal C≡C moiety to the other.

Unfortunately, all attempts to convert **6**$^+BF_4^-$ to a σ complex of the formula $(\eta^5\text{-}C_5Me_5)Re(NO)(PPh_3)(C{\equiv}CC{\equiv}CC{\equiv}CC{\equiv}CX)$(X = $SiMe_3$ or H) have been unsuccessful. Indeed, we are unable to effect *any* clean transformation of **6**$^+BF_4^-$, as assayed by the multitude of ^{31}P NMR signals commonly observed prior to workup. These include reactions with MeOH, $MeOH/K_2CO_3$, *t*-BuOK, MeLi, and many other potential desilylating or protodesilylating reagents. We speculate that the rhenium must ligate to a terminal C≡CX moiety prior to formation of a σ complex. Based upon the slow interconversion of **IV** and **V**, this might entail a much higher energy barrier than other available reaction pathways.

However, $Me_3SiC{\equiv}CC{\equiv}CC{\equiv}CC{\equiv}CSiMe_3$ may prove to be a useful building block with more labile metal fragments. An alternative strategy would be to first selectively react *one* of the termini of $Me_3SiC{\equiv}CC{\equiv}CC{\equiv}CC{\equiv}CSiMe_3$ to obtain a differentially functionalized polyyne, as was done with $Me_3SiC{\equiv}CC{\equiv}CSiMe_3$ in Scheme 1. For example, a monolithium derivative would likely be of considerable utility. However, all investigations to date appear to give near-statistical mixtures of difunctionalized, monofunctionalized, and unfunctionalized compounds. Finally, attempts to generate a σ complex by the direct condensation of $Me_3SiC{\equiv}CC{\equiv}CC{\equiv}CC{\equiv}CSiMe_3$ and the methoxy complex $(\eta^5\text{-}C_5Me_5)Re(NO)(PPh_3)(OMe)$ also give numerous products.

The Cadiot-Chodkiewicz reaction

The Eglinton reaction is most productively applied to the *symmetrical* coupling of identical terminal alkynes. *Cross* couplings of unlike alkynes normally give mixtures of products [5c]. However, special alkyne cross-coupling protocols have been devised. Of these, the Cadiot-Chodkiewicz reaction is the most frequently utilized [8, 9, 13]. One educt is commonly a *halo*alkyne, and the other is some type of alkynyl copper species. The latter is typically generated in situ from a terminal alkyne, amine base, and copper (I) salt. We therefore sought to apply this procedure within the coordination sphere of **I**. In this context, we had previously demonstrated that both **1** and **2** react with *n*-BuLi to give the corresponding $ReC{\equiv}CLi$ and $ReC{\equiv}CC{\equiv}CLi$ species [6a], another type of reaction that is well-known for organic terminal alkynes.

A variety of coupling conditions have been investigated. Superior results are obtained when **2** is first quantitatively converted to an alkynyl copper species. As shown in Scheme 4, this is accomplished by the sequential addition of *n*-BuLi and CuI (THF, –45 to –20 °C) [5d]. After a brief period at room temperature, ^{31}P NMR spectra show broad signals indicating complete conversion

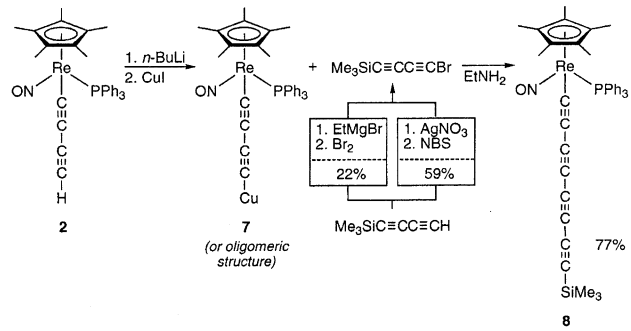

Scheme 4. – Synthesis of a rhenium octatetraynyl complex by a Cadiot-Chodkiewicz coupling reaction.

to a new complex or mixture of complexes. These are presumed to have the empirical formula (η^5-C_5Me_5)Re(NO)(PPh_3)(C≡CC≡CCu) (**7**). IR spectra also show new bands (cm^{-1}, THF: $\nu_{C\equiv C}$ 2010 m br, ν_{NO} 1650 vs). Complex **7** is isolable, and additional properties will be described in a future publication.

The brominated diyne $Me_3SiC\equiv CC\equiv CBr$ [14] can be synthesized from $Me_3SiC\equiv CC\equiv CH$ by the two routes shown in Scheme 4. The $EtMgBr/Br_2$ sequence, which has been used to brominate other terminal alkynes [15], affords only a 22% yield. Some improvement is possible with *n*-BuLi/Br_2 [14]. However, the $AgNO_3$/NBS sequence gives much higher yields [16, 17]. This recipe is capable of brominating both silylated and terminal alkynes [16], and high selectivities are achieved with the solvent combination described in the experimental section. Regardless, $Me_3SiC\equiv CC\equiv CBr$ is a labile compound that shows significant decomposition after one week at 0 °C, even when stored as a dilute stock solution. In contrast, solutions of $Me_3SiC\equiv CC\equiv CH$ can be kept for weeks at 0 °C with only slight decomposition.

THF solutions of **7** are then treated with $EtNH_2$ (excess, –20 °C) and $Me_3SiC\equiv CC\equiv CBr$ (1.1 equiv) as shown in Scheme 4. Workup gives the analytically pure 1,3,5,7-tetrayne (η^5-C_5Me_5)Re(NO)-(PPh_3)(C≡CC≡CC≡CC≡$CSiMe_3$) (**8**) in 77% yield after crystallization [5d]. The brominated monoyne $Et_3SiC\equiv CBr$, which is considerably more robust than $Me_3SiC\equiv CC\equiv CBr$, undergoes an analogous coupling reaction to give a 1,3,5-hexayne [5d].

Complex **8** exhibits spectroscopic properties similar to those of lower homologs reported earlier. However, IR spectra show additional and much more intense $\nu_{C\equiv C}$ bands (cm^{-1}, THF/KBr: $\nu_{C\equiv C}$ 2115/2107 m, 2069/– m sh/–, 2046/2045 vs, 1971/1968 s, ν_{NO} 1660/1650 s). Interestingly, the chemical shifts of the $ReC\equiv C\mathit{C}\equiv \mathit{C}\mathit{C}\equiv \mathit{C}\mathit{C}\equiv CSi$ ^{13}C NMR signals cluster in the narrow range of 66.5-64.7 ppm (C_6D_6). This suggests a gradual convergence toward a limiting value associated with polymeric "carbyne" [4]. Complex **8** gradually decomposes without melting at 225-350 °C, as assayed by IR and MS. The resulting solid is insoluble in all common solvents, but exhibits new, very broad IR $\nu_{C\equiv C}$ and ν_{NO} bands (cm^{-1}, KBr: 1994 and 1655).

There are few if any previous applications of the Cadiot-Chodkiewicz reaction in the coordination sphere of a transition metal [18]. The preceding transformations establish a vocabulary and syntax of coupling/deprotection procedures that can be applied in an iterative fashion. For example, **8** can be converted to the parent 1,3,5,7-tetraynyl complex (η^5-C_5Me_5)Re(NO)(PPh_3)(C≡CC≡CC≡CC≡CH), which is then oxidatively dimerized by the Eglinton reaction in a sequence parallel to that given in Schemes 1 and 2. This gives a homolog of **5** with a C_{16} chain. To date, homologs with up to C_{20} chains have been prepared [5d]. Full details of these reactions, which have been communicated [5d] but are still being optimized, will be given in a later publication.

Crystal structure of the 1,3,5,7-tetrayne 8

There has been conjecture that long polyalkynyl or "carbyne" fragments may be precursors to buckyballs such as C_{60} [4]. This would require chain curvature, consistent with the low bending force constants of alkynes [19]. As such, it is of interest to probe for any solid state deformations in model polyalkynes. Thus, the crystal structure of **8** has been determined as outlined in Table I and the *Experimental section*. Refinement gives the atomic coordinates in Table II, the molecular structure in Figure 1, and the bond lengths and angles in Table III.

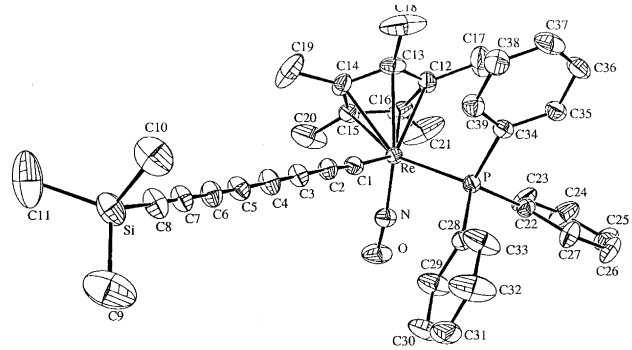

Figure 1. – The molecular structure of (η^5-C_5Me_5)Re(NO)(PPh_3)-(C≡CC≡CC≡CC≡$CSiMe_3$) (**8**).

Table I. – Summary of crystallographic data for (η^5-C_5Me_5)Re(NO)-(PPh_3)(C≡CC≡CC≡CC≡$CiMe_3$) (**8**).

molecular formula	$C_{39}H_{39}NOPReSi$
molecular weight	783.01
crystal system	monoclinic
space group	$P2_1/n$ (No. 14)
cell dimensions (16 °C)	
a, Å	16.685(5)
b, Å	13.211(2)
c, Å	18.067(4)
β, deg	109.97(2)
V, Å^3	3743(2)
Z	4
d_{calc}, g/cm^3	1.389 (16 °C)
d_{obs}, g/cm^3 (Et_2O/CH_2I_2)	1.383 (22 °C)
crystal dimensions, mm	0.31 x 0.30 x 0.22
diffractometer	CAD4
radiation λ, Å	Mo Kα (0.71073)
data collection method	θ-2θ

scan speed, deg/min	variable
reflections measured	7150
range/indices (h, k, l)	0, –15 ; 0, –14 ; –21, 21
scan range	$0.80 + 0.34 \tan \theta$
2θ limit, deg	4.00–50.00
no. of reflections between std	98
total no. of unique data	6577
no. of observed data, $I > 3\ \sigma(I)$	4466
abs. coefficient, cm^{-1}	33.906
min. transmission, %	83.47
max. transmission, %	99.98
no. of variables	397
goodness of fit	1.222
no. of observed data averaged	359
R (averaging) (I_{obs}, F_{obs})	0.018, 0.016
$R = \Sigma \|\|F_0\| - \|F_c\|\|/\Sigma\|F_0\|$	0.0329
$R_W = \Sigma \|\|F_0\| - \|F_c\|\|w^{1/2}/\Sigma\|F_0\|w^{1/2}$	0.0425
Δ/σ (max)	0.010
Δ/ρ (max), e/Å^3	1.185 (ca. 1.60 Å from Re)

Table II. – Atomic coordinates and equivalent isotropic thermal parameters of located atoms in **8** [35].

Atom	x	y	z	B (Å^2)
Re	0.02849(1)	0.20865(2)	0.21457(1)	3.549(4)
P	0.0108(1)	0.1366(1)	0.32881(8)	3.87(3)
Si	0.4637(2)	0.8688(2)	0.7008(1)	7.10(7)
O	–0.1443(3)	0.2916(5)	0.1496(3)	8.4(2)
N	–0.0753(3)	0.2602(5)	0.1822(3)	5.1(1)
C1	0.0933(4)	0.3197(5)	0.2887(3)	4.3(1)
C2	0.1357(4)	0.3845(5)	0.3317(4)	4.6(2)
C3	0.1799(4)	0.4578(5)	0.3804(4)	5.1(2)
C4	0.2184(5)	0.5258(5)	0.4228(4)	5.4(2)
C5	0.2639(4)	0.5975(5)	0.4738(4)	5.3(2)
C6	0.3043(5)	0.6594(5)	0.5196(4)	5.3(2)
C7	0.3535(5)	0.7246(5)	0.5755(4)	5.3(2)
C8	0.3960(5)	0.7810(5)	0.6257(5)	6.4(2)
C9	0.4000(8)	0.933(1)	0.7427(8)	15.0(5)
C10	0.5439(7)	0.7940(7)	0.7734(7)	10.0(3)
C11	0.5144(9)	0.9567(8)	0.6521(6)	14.1(4)
C12	0.0768(4)	0.0680(5)	0.1662(4)	5.5(2)
C13	0.1446(4)	0.1346(6)	0.1967(4)	5.9(2)
C14	0.1254(5)	0.2244(5)	0.1513(4)	6.1(2)
C15	0.0423(5)	0.2101(6)	0.0930(4)	5.8(2)
C16	0.0151(4)	0.1146(6)	0.1039(3)	5.8(2)
C17	0.0831(7)	–0.0393(7)	0.1919(6)	12.7(3)
C18	0.2301(6)	0.111(1)	0.2555(6)	14.4(4)
C19	0.1846(6)	0.3124(8)	0.1565(6)	13.4(3)
C20	–0.0041(8)	0.2800(9)	0.0289(5)	13.9(3)
C21	–0.0649(6)	0.065(1)	0.0539(5)	14.7(4)
C22	–0.0755(4)	0.0470(5)	0.3126(3)	4.4(1)
C23	–0.1151(5)	0.0079(7)	0.2396(4)	7.1(2)
C24	–0.1785(5)	–0.0647(8)	0.2255(5)	9.5(3)
C25	–0.2036(5)	–0.0987(7)	0.2851(5)	8.4(2)
C26	–0.1668(5)	–0.0600(7)	0.3584(5)	7.8(2)
C27	–0.1031(5)	0.0127(7)	0.3716(4)	6.7(2)
C28	–0.0117(4)	0.2268(5)	0.3964(3)	4.5(2)
C29	–0.0709(6)	0.2972(7)	0.3696(5)	8.5(2)
C30	–0.0889(6)	0.3657(8)	0.4203(5)	10.3(3)
C31	–0.0490(5)	0.3636(7)	0.4962(5)	8.5(2)
C32	0.0104(8)	0.2971(9)	0.5230(5)	12.8(3)
C33	0.0293(7)	0.2276(8)	0.4747(5)	9.8(3)
C34	0.1062(4)	0.0675(5)	0.3906(3)	4.4(1)
C35	0.1039(4)	–0.0346(5)	0.4063(4)	5.3(2)
C36	0.1775(5)	–0.0833(6)	0.4523(5)	6.9(2)
C37	0.2512(5)	–0.0300(7)	0.4834(5)	7.7(2)
C38	0.2529(5)	0.0705(7)	0.4693(5)	6.8(2)
C39	0.1803(4)	0.1199(6)	0.4225(4)	5.7(2)

Table III. – Selected bond lengths (Å), bond angles (deg), and torsion-type angles (deg) in **8**.

Bond lengths			
Re–P	2.381(2)	C3–C4	1.21(1)
Re–N	1.764(6)	C4–C5	1.36(1)
Re–C1	2.032(7)	C5–C6	1.194(9)
Re–C12	2.313(7)	C6–C7	1.37(1)
Re–C13	2.289(7)	C7–C8	1.20(1)
Re–C14	2.286(7)	C8–Si	1.848(9)
Re–C15	2.285(7)	Si–C9	1.72(2)
Re–C16	2.299(7)	Si–C10	1.81(1)
C1–C2	1.208(9)	Si–C11	1.83(1)
C2–C3	1.35(1)	N–O	1.175(7)
Bond angles			
P–Re–N	92.5(2)	C8–Si–C9	108.4(6)
Re–N–O	170.0(6)	C8–Si–C10	107.7(4)
P–Re–C1	85.0(2)	C8–Si–C11	108.2(5)
N–Re–C1	100.4(3)	C9–Si–C10	111.3(7)
Re–C1–C2	176.4(6)	C9–Si–C11	110.9(8)
C1–C2–C3	177.4(8)	C10–Si–C11	110.2(7)
C2–C3–C4	178.2(8)	Re–P–C22	116.6(2)
C3–C4–C5	176.4(8)	Re–P–C28	115.6(2)
C4–C5–C6	178.9(8)	Re–P–C34	112.7(2)
C5–C6–C7	175.9(8)	C22–P–C28	101.6(3)
C6–C7–C8	179(1)	C22–P–C34	104.4(3)
C7–C8–Si	178.0(9)	C28–P–C34	104.4(3)
Torsion-type angles			
P–Re–Si–C9	–63.0(5)	N–Re–Si–C9	28.1(6)
P–Re–Si–C10	56.1(4)	N–Re–Si–C10	147.2(4)
P–Re–Si–C11	174.0(5)	N–Re–Si–C11	–94.9(5)

Although many structural features of **8** merit analysis, most *molecular* properties are in our opinion unexceptional. First, as is obvious from Figure 1, the *sp* carbon chain does not exhibit what we view as appreciable bending. The bond angles in the ten-atom ReC≡CC≡CC≡CC≡CSi unit range from 175.9(8)° to 179(1)°. However, the carbon thermal ellipsoids appear to increase slightly with greater distance from rhenium, as evidenced by the B(Å^2) values in Table II. This may be due to some librational motion. Second, the lengths of the carbon-carbon triple bonds range from 1.194(9) to 1.21(1) Å, typical distances for alkynes [20]. Third, the carbon-carbon single bonds are much shorter

Table IV. – Anisotropic thermal parameters for **8** [36].

Atom	*U*(1,1)	*U*(2,2)	*U*(3,3)	*U*(1,2)	*U*(1,3)	*U*(2,3)
Re	0.0515(1)	0.0438(1)	0.0419(9)	0.0017(1)	0.0190(7)	–0.0006(1)
P	0.0584(8)	0.0494(9)	0.0418(7)	0.0006(8)	0.0206(5)	–0.0007(7)
Si	0.108(2)	0.061(1)	0.080(1)	–0.003(1)	0.004(1)	–0.018(1)
O	0.068(3)	0.154(5)	0.087(3)	0.048(3)	0.013(3)	0.019(4)
N	0.066(3)	0.079(4)	0.049(3)	0.012(3)	0.020(2)	0.004(3)
C1	0.065(3)	0.055(4)	0.049(3)	0.011(3)	0.023(2)	0.006(3)
C2	0.060(3)	0.052(4)	0.060(3)	–0.006(3)	0.017(3)	–0.003(3)
C3	0.071(4)	0.053(4)	0.064(4)	0.001(3)	0.017(3)	0.004(3)
C4	0.077(4)	0.056(4)	0.060(4)	–0.005(4)	0.008(3)	0.000(3)
C5	0.068(4)	0.057(4)	0.068(4)	0.004(4)	0.010(3)	0.001(3)
C6	0.071(4)	0.054(4)	0.065(4)	–0.009(4)	0.009(3)	0.001(3)
C7	0.074(4)	0.051(4)	0.066(4)	0.001(3)	0.011(3)	0.005(3)
C8	0.094(5)	0.056(4)	0.078(5)	0.001(4)	0.008(4)	0.002(4)
C9	0.15(1)	0.20(1)	0.17(1)	0.05(1)	–0.011(9)	–0.05(1)
C10	0.126(8)	0.108(7)	0.110(7)	–0.007(7)	–0.006(6)	–0.034(6)
C11	0.29(1)	0.109(7)	0.102(7)	–0.096(8)	0.021(8)	– 0.028(6)
C12	0.110(4)	0.048(4)	0.070(3)	0.001(3)	0.055(3)	–0.008(3)
C13	0.075(4)	0.099(5)	0.057(3)	0.022(4)	0.033(2)	–0.013(4)
C14	0.104(4)	0.059(4)	0.095(4)	–0.023(3)	0.068(3)	–0.022(3)
C15	0.104(4)	0.076(4)	0.057(3)	0.029(4)	0.051(2)	0.017(3)
C16	0.067(3)	0.103(5)	0.057(3)	–0.015(4)	0.031(2)	–0.034(3)
C17	0.308(8)	0.064(6)	0.196(5)	0.019(6)	0.196(4)	0.003(5)
C18	0.104(5)	0.36(2)	0.084(5)	0.100(8)	0.035(4)	0.001(9)
C19	0.229(6)	0.147(8)	0.215(6)	–0.110(5)	0.181(4)	–0.092(6)
C20	0.250(8)	0.22(1)	0.087(4)	0.147(7)	0.101(4)	0.069(6)
C21	0.123(6)	0.34(1)	0.114(5)	–0.077(8)	0.068(4)	–0.145(6)
C22	0.061(3)	0.058(4)	0.056(3)	–0.001(3)	0.027(2)	–0.002(3)
C23	0.092(4)	0.118(6)	0.082(4)	–0.039(4)	0.057(3)	–0.032(4)
C24	0.110(5)	0.158(8)	0.118(5)	–0.055(5)	0.069(4)	–0.069(5)
C25	0.086(4)	0.100(6)	0.156(6)	–0.029(4)	0.071(3)	–0.018(6)
C26	0.092(4)	0.124(6)	0.099(4)	–0.028(4)	0.054(3)	0.022(5)
C27	0.093(4)	0.100(6)	0.067(4)	–0.021(4)	0.036(3)	0.009(4)
C28	0.072(3)	0.056(4)	0.048(3)	0.003(3)	0.026(2)	–0.004(3)
C29	0.125(6)	0.133(7)	0.055(4)	0.060(5)	0.019(4)	–0.009(5)
C30	0.163(6)	0.148(7)	0.084(5)	0.105(5)	0.045(4)	0.017(5)
C31	0.131(5)	0.110(6)	0.101(4)	0.022(5)	0.063(3)	–0.029(5)
C32	0.170(8)	0.219(9)	0.076(5)	0.074(7)	0.015(5)	–0.077(5)
C33	0.151(7)	0.138(7)	0.061(5)	0.074(5)	0.007(5)	–0.016(5)
C34	0.063(3)	0.060(4)	0.043(3)	0.011(3)	0.018(2)	–0.000(3)
C35	0.073(4)	0.061(4)	0.068(4)	0.011(3)	0.027(3)	0.000(3)
C36	0.098(5)	0.069(5)	0.094(5)	0.036(4)	0.033(4)	0.019(4)
C37	0.084(5)	0.118(6)	0.075(5)	0.050(4)	0.007(4)	0.010(5)
C38	0.062(4)	0.103(6)	0.077(5)	–0.004(4)	0.002(4)	0.011(5)
C39	0.066(4)	0.076(5)	0.067(4)	0.003(4)	0.012(3)	0.007(4)

than that in ethane (1.35(1)–1.37(1) vs. 1.54 Å) [20]. However, such contractions are usual with conjugated polyynes [4, 17, 20-23], as the bonds are comprised of two *sp*-hybridized orbitals, instead of sp^3-hybridized orbitals. Fourth, the rhenium-carbon bond length is very close to those in a μ-butadiynediyl (ReC≡CC≡CRe) complex of **I** reported previously (2.032(7) vs. 2.037(5) Å) [5a, 6b]. Fifth, the ≡C–Si bond length is similar to those in $Me_3SiC{\equiv}CC{\equiv}CC{\equiv}CC{\equiv}CSiMe_3$ (1.848(9) vs. 1.819(7)-1.822(7) Å) [22]. Finally, the distance between the rhenium and silicon endgroups is 12.743(2) Å.

Additional structural features of **8** have been examined. First, a Newman-type projection down the silicon-rhenium axis is shown in Figure 2. This illustrates the relationships between substituents on the endgroups, which define torsion-type angles as summarized in Table III. When **8** is viewed on a stereoscopic screen with atoms set at van der Waals radii, it is obvious that

there is no steric communication between the termini. However, the torsion angles are reminiscent of those in alkyl complexes of the cyclopentadienyl fragment (η^5-C_5H_5)Re(NO)(PPh_3), for which steric interactions are important conformational determinants [24]. It should also be noted that **I** is a strong π base, with a *d*-orbital HOMO lying in a plane that contains the rhenium-phosphorus bond and is perpendicular to the rhenium-nitrogen bond [24a]. This is of proper symmetry to backbond, through the tetrayne assembly, into the Si–C11 σ^* orbital of **8**.

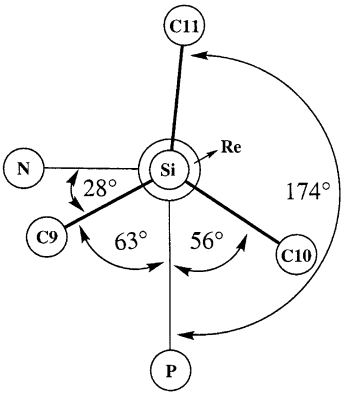

Figure 2. – Newman-type projection down the silicon-rhenium axis in **8**.

The unit cell contains four molecules in paired orientations. Packing diagrams are given in Figure 3, and show that the molecules within each pair have (1) approximately parallel chains, (2) head-to-tail arrangements, and (3) opposite absolute configurations at rhenium. The closest carbon-carbon distance between the parallel chains is 7.78 Å (C3–C8′ and C8–C3′), and additional spacings are given pictorially in Figure 4. The midpoints of the C4–C5 and C4′–C5′ bonds approximate the "centers" of the chains, and are separated by 8.35 Å. The difference between these values (8.35 vs. 7.78 Å) reflects the degree by which the chains are "offset" or out-of-registry. The distances should be nearly identical when the endgroups are exactly aligned. Alternatively, the offset is roughly "two carbons" as judged by the atoms with the closest contacts or a visual inspection of Figure 4.

The two pairs of molecules in the unit cell are mutually orthogonal, and extend through the lattice as illustrated by the views in Figure 3. With appropriate perspectives, a "herringbone" or "zig-zag" motif is apparent (Fig. 3c) [25]. Sometimes it misleadingly appears that neighboring parallel chains have head-to-head orientations. Hence, one stereoscopic view is included (Fig. 3c). Interestingly, the closest carbon-carbon contacts involve perpendicular chains (6.26 Å, C2–C8″). This is illustrated by the arrows and darkened atoms in Figure 3b.

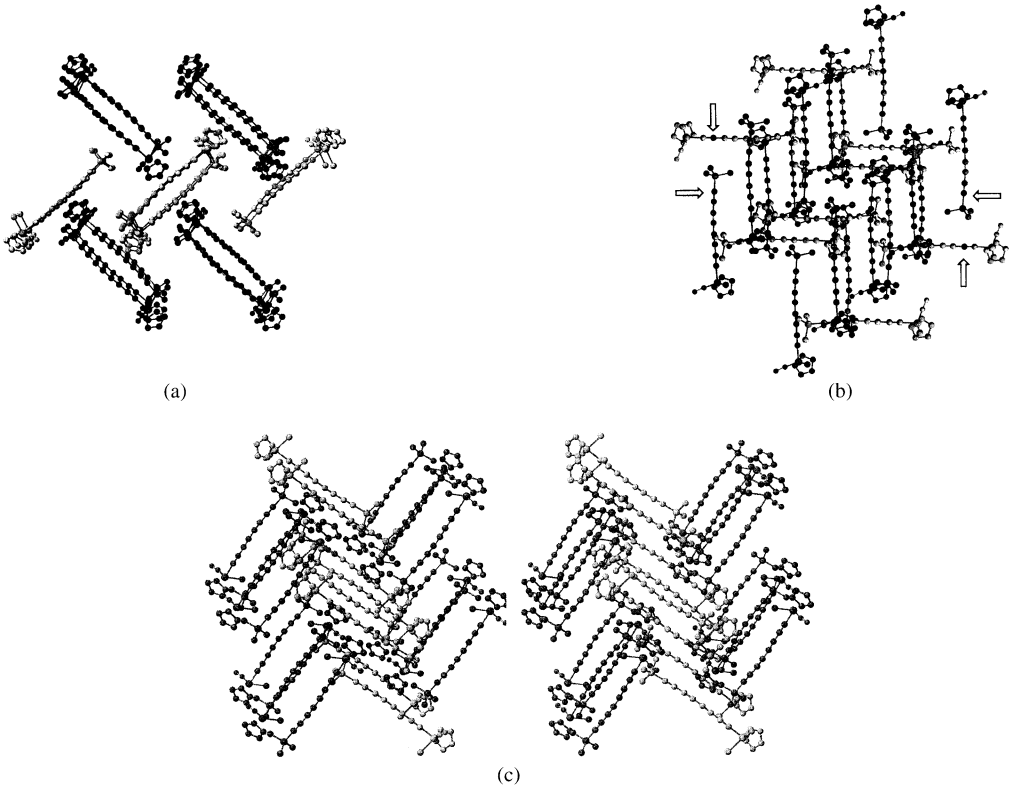

Figure 3. – Representative packing diagrams for crystalline **8** (phenyl and C*Me* groups have been omitted for clarity).

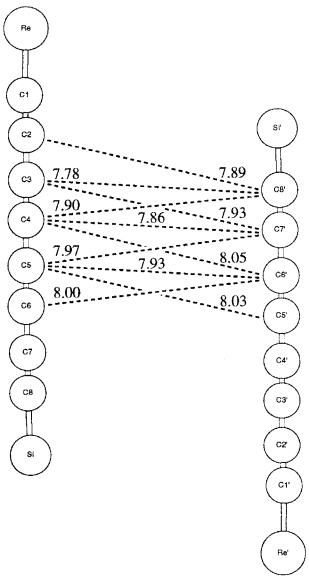

Figure 4. – Summary of distances between approximately parallel carbon chains in crystalline **8**.

Crystal structures of other 1,3,5,7-tetraynes

Structural data for all crystallographically characterized 1,3,5,7-tetraynes that we have been able to locate are summarized in Table V [4, 17, 21-23, 26]. The *sp*-carbon chains in these six compounds, which include one pentayne, exhibit bond lengths and angles similar to those of **8** (C–C range, 1.32–1.39 Å; C≡C range, 1.172-1.22 Å; angle range, 174°–179.4°). All show a very high degree of linearity, as evidenced by the close correspondence of the C1–C8 distances (computed from atomic coordinates when available) and the sums of the C1–C8 bond lengths (≤0.4% difference). The average bond angles range from a high of 178.4° for the pentayne PhC≡CC≡CC≡CC≡CC≡CPh ("most linear") through 177.5° for **8** to a low of 176.7° for the tetrayne with cyclobutadienyl cobalt endgroups ("most bent"). When these molecules are viewed on a stereoscopic screen, *t*-BuC≡CC≡CC≡CC≡C-*t*-Bu and $Me_3SiC{\equiv}CC{\equiv}CC{\equiv}CC{\equiv}CSiMe_3$ show the most aesthetically pleasing "bowing" or gradual, uniform curvature. In contrast, the cobalt-containing tetrayne exhibits a slight step kink in the middle of the chain.

In the case of pentayne PhC≡CC≡CC≡CC≡CC≡CPh, the crystal lattice is also comprised of two approximately orthogonal sets of parallel chains ($Z=2$) [17]. In appropriate perspectives, distinctive layers are apparent (ca. 4.6 Å separation). The closest distance between carbons on parallel chains is 3.645 Å (C1–C7′; carbon atom numbering as in Figure 4), and the center-to-center spacing is 5.218 Å. The difference between these values is much larger than for **8** (≥1.4 vs. ≤0.6 Å), indicating that the chains are offset by a greater degree (ca. three carbon atoms). When the unit cell is viewed with atoms set at van der Waals radii, the chains gently osculate, leaving little or no gap. The closest distance between carbons on non-parallel chains is 5.43 Å (C1–C9").

The tetraynes *t*-BuC≡CC≡CC≡CC≡C-*t*-Bu and Me_3Si-C≡CC≡CC≡CC≡$CSiMe_3$ have sterically similar endgroups. As summarized in Table V, they crystallize in identical orthorhombic space groups ($Z=8$) with nearly the same unit cell dimensions [4, 22]. As expected, the *t*-butyl carbon-carbon bonds are 0.30–0.36 Å shorter than the trimethylsilyl silicon-carbon bonds. Accordingly, the unit cell volume of *t*-BuC≡CC≡CC≡CC≡C-*t*-Bu is slightly smaller. These molecules pack in a somewhat more complex manner, with four different sets of parallel chains. It is not possible from any perspective to simultaneously display all chains in a fully elongated fashion (i.e., in planes parallel to that of the paper as in Figure 3). The closest distances between carbons on parallel chains are 4.02 and 3.85 Å (C3–C4′ and C3–C3′), while the center-to-center spacings are 5.04 and 5.17 Å. These data indicate a chain offset of ca. three carbon atoms, with a separation slightly greater than the sum of the *sp*-carbon van der Waals radii. As with **8**, carbons on non-parallel chains give the closest contacts (3.50 and 3.59 Å, C2–C2″).

The tetrayne with cyclobutadienyl cobalt endgroups crystallizes with two approximately orthogonal sets of parallel chains, as observed for **8** and PhC≡CC≡C-C≡CC≡CC≡CPh [23]. The closest distance between carbons on parallel chains is 7.09 Å (C2–C2′), and the center-to-center spacing is 9.85 Å. These data indicate a chain offset of ca. five carbon atoms, the most pronounced of all compounds in Table V. The closest contact between carbons on non-parallel chains is 7.61 Å (C1–C4″). Taken together, the preceding data show that the bulky cobalt- and rhenium-containing endgroups enforce much larger chain-chain separations than the others (7.78-7.09 or 8.35-9.85 Å vs. 3.50–3.85 or 5.02–5.22 Å), much larger than the sum of the *sp*-carbon van der Waals radii [27]. However, the chains in **8** are offset the least of all compounds in Table V. We speculate that this is primarily due to the more intimate nesting possible with sterically unlike endgroups, a feature that is unique to **8**.

In conclusion to the structural part of this investigation, it is obvious that there will be a rapid growth of polyalkynyl compounds in the literature, together with attendant crystallographic studies [28]. The data and analyses presented herein, which involve both new and previously reported molecules, should provide a valuable framework for the interpretation of many physical, and even chemical, properties. For example, there is believed

Table V. – Summary of bond lengths (Å), bond angles (deg), and other data for crystallographically characterized 1,3,5,7-tetraynes XC≡CC≡CC≡CC≡CX′. [a]

X/X′	Ph/Ph [b, c]	Ph/C≡CPh [d, e]	*t*-Bu/*t*-Bu	Me_3Si/Me_3Si	Cycbu/Cycbu [f]	**8**
Bond lengths						
C1–C2	1.19	1.192	1.217(9)	1.20(1)	1.19(2)	1.208(9)
C2–C3	1.36	1.369	1.377(9)	1.39(1)	1.38(3)	1.35(1)
C3–C4	1.22	1.206	1.172(8)	1.20(1)	1.18(2)	1.21(1)
C4–C5	1.32	1.368	1.351(9)	1.33(1)	1.38(4)	1.36(1)
C5–C6	1.22	1.208	1.218(9)	1.20(1)	1.18(2)	1.194(9)
C6–C7	1.36	1.368	1.36(1)	1.378(9)	1.38(3)	1.37(1)
C7–C8	1.19	1.206	1.202(8)	1.209(9)	1.19(2)	1.20(1)
C1–C8 distance	–	8.915	8.87	8.88	8.86	8.872(9)
sum of C1–C8 bond lengths	8.86	8.917	8.90	8.91	8.88	8.89
Bond angles [b]						
X–C1–C2	–	178.08(6)	178.8(6)	178.1(6)	176(2)	176.4(6)
C1–C2–C3	–	178.49	177.6(6)	177.7(8)	177(3)	177.4(8)
C2–C3–C4	–	178.30	178.5(5)	177.4(7)	179(3)	178.2(8)
C2–C4–C5	–	178.67	177.4(6)	177.8(8)	174(3)	176.4(8)
C4–C5–C6	–	178.52	176.7(6)	176.9(8)	174(3)	178.9(8)
C5–C6–C7	–	178.52	178.9(6)	178.4(7)	179(3)	175.9(8)
C6–C7–C8	–	178.67	176.1(6)	178.6(7)	177(3)	179(1)
C7–C8–X′	–	178.30	179.4(6)	177.2(6)	176(2)	178.0(9)
av. angle	–	178.4	177.9	177.8	176.7	177.5
Other data						
space group	$P2_1/a$	$P2_1/n$	*Pbcn*	*Pbcn*	$P2_1/c$	$P2_1/n$
a, Å	17.74	8.805	11.185	11.966	13.950	16.685
b, Å	3.99	5.218	11.781	12.544	9.848	13.211
c, Å	10.78	17.127	22.36	22.809	18.435	18.067
β, deg	110.5	94.563	–	–	106.269	109.97
V, Å^3	715	784	2947(4)	3 423.7	3417(2)	3 743.10
Z	2	2	8	8	2	4
d_{calc}, g/cm^3	1.16	1.16	0.95	0.94	1.201	1.389
ref	21	17	4	22	23	this work

[a] All esd values are as reported in the citation provided, or rounded downward by one significant digit. [b] No bond angles or atomic coordinates were reported for X/X′ = Ph/Ph. [c] Unit cell parameters have been reported for two forms of crystals. Data for the second form: space group $P2_1/a$; $a = 19.5$ Å, $b = 9.08$ Å, $c = 3.95$ Å; $\beta = 99°$; $Z = 2$ [21b]; $V = 691$ Å^3; $d_{calc} = 1.20$ g/cm^3. [d] Additional data for diphenyl 1,3,5,7,9-pentayne: C8–C9 1.369 Å; C9–C10 1.192 Å; ∠C8–C9–C10 178.49°; ∠C9–C10–Ph 178.08(6)°. [e] Other unit cell parameters have also been reported: space group $P2_1/a$; $a = 17.5$ Å, $b = 5.12$ Å, $c = 9.25$ Å; $\beta = 112°$; $Z = 2$ [21b]. [f] Cycbu = (η^5-C_5H_5)Co(η^4-C(SiMe$_3$)=C(SiMe$_3$)-C(SiMe$_3$)=C).

to be some correlation between chain spacing and the thermal stabilities or explosive properties of polyalkynyl compounds [4]. Finally, syntheses of additional types of complexes that contain chiral rhenium endgroups and long *sp*-carbon chains will be reported in the near future.

Experimental section

General data

All instrumentation, general procedures, and solvent or reagent purifications were identical with those described earlier [6a]. Solvents or reagents not given previously: toluene, distilled from Na; acetone, distilled from anhydrous $CaSO_4$; CuI (99.999%, Aldrich), $EtNH_2$ (anhydrous, 99%, Aldrich), $Me_3SiC{\equiv}CC{\equiv}CSiMe_3$ (Farchan), $AgNO_3$ (99+%, Spectrum), and NBS (Aldrich), used as received from commercial suppliers; EtMgBr (3.0 M in ether, Aldrich) [29] and MeLi · LiBr (1.5 M in ether, Aldrich) [30], standardized by literature procedures.

(η^5-C_5Me_5)Re(NO)(PPh_3)(C≡CC≡CC≡C-C≡CSiMe_3) **8**

A Schlenk flask was charged with **1** (0.0684 g, 0.103 mmol) [6a] and THF (5 mL) and cooled to –45 °C (CO_2/CH_3CN). Then *n*-BuLi (2.2 M in hexane, 52 mL, 0.113 mmol) was added with stirring. After

2 h, the cold bath was warmed to –20 °C with additional CH_3CN and freshly ground CuI (0.0196 g, 0.103 mmol) was added. The cold bath was removed and the mixture allowed to warm. After 15 min at room temperature, the mixture was cooled to –20 °C, and $EtNH_2$ (ca. 0.5 mL) was added. A solution of freshly distilled $Me_3SiC{\equiv}CC{\equiv}CBr$ (0.0228 g, 0.113 mmol) in THF (2 mL) was added dropwise. After 10 min, the solvent was removed by oil pump vacuum. The residue was extracted with toluene (2 × 3 mL). The extract was filtered through a 2-cm silica gel pad [31]. Solvent was removed from the bright red-orange filtrate by oil pump vacuum. The residue was dissolved in a minimum of toluene (ca. 1 mL), and hexane was added (ca. 10 mL). The mixture was kept at –40 °C for 16 h. The dark red crystals were collected by filtration and dried by oil pump vacuum to give **8** (0.062 g, 0.079 mmol, 77%), dec 225-350 °C (gradual, without melting; see text). Anal calc for $C_{39}H_{39}NOPReSi$: C, 59.82; H, 5.02. Found: C, 60.00; H, 5.12. IR (cm^{-1}, THF/CH_2Cl_2/KBr): $\nu_{C{\equiv}C}$ 2115/2114/2107 m, 2069/2067/– m sh/m sh/–, 2046/2046/2045 vs, 1971/1969/1968 s, ν_{NO} 1660/1656/1650 s. ^1H NMR (δ, C_6D_6): 7.64–7.58 (m, 6H of $3C_6H_5$), 7.03–6.95 (m, 9H of $3C_6H_5$), 1.49 (s, $C_5(CH_3)_5$), 0.003 (s, $Si(CH_3)_3$). $^{13}C\{^1H\}$ NMR (ppm, C_6D_6) [32]: 135.5 (d, J_{CP} = 51.9 Hz, *i*-Ph), 134.5 (d, J_{CP} = 10.8 Hz, *o*-Ph), 130.8 (s, *p*-Ph), 128.8 (d, J_{CP} = 10.9 Hz, *m*-Ph), 117.6 (d, J_{CP} = 15.9 Hz, Re*C*≡C), 113.4 (s, ReC≡*C*), 101.5 (s, $C_5(CH_3)_5$), 90.8, 87.0 (2 s, *C*≡CSi), 66.5 (d, J_{CP} = 2.9 Hz, ReC≡C*C*), 65.9, 65.5, 64.7 (3 s, ReC≡CC≡*CC*≡*C*), 10.28 (s, $C_5(CH_3)_5$), 0.0 (s, $SiCH_3$). $^{31}P\{^1H\}$ NMR (ppm, C_6D_6): 17.4 (s). MS (*m/z*, EI, 30 eV) 783 ($\mathbf{8}^+$, 100%), 262 (PPh_3^+, 43%); no other peaks >5% above 200. UV-vis (nm, CH_2Cl_2, 6.3×10^{-5} M (ϵ, M^{-1} cm^{-1})) 234 (31400), 242 sh (30500), 266 sh (20700), 322 sh (17800), 344 (27600), 394 sh (8800), 328 sh (5700), 466 sh (3800).

$Me_3SiC{\equiv}CC{\equiv}CH$ [10]

A Schlenk flask was charged with $Me_3SiC{\equiv}CC{\equiv}CSiMe_3$ (10 g, 0.051 mol) and ether (150 mL). Then MeLi·LiBr (1.5 M in ether, 38 mL, 0.057 mol) was added with stirring. After 24 h, the dark-green mixture was slowly poured into a 0 °C saturated aqueous NH_4Cl solution (300 mL). The resulting aqueous phase was extracted with pentane (3 x 50 mL), and the combined organic phases were dried over Na_2SO_4. The solvents were removed by rotary evaporation below room temperature, and the residue was vacuum transferred to give $Me_3SiC{\equiv}CC{\equiv}CH$ as a colorless liquid (4.15–5.05 g, 0.034–0.041 mol, 66-72%) that was stored in a freezer. IR (cm^{-1}, pentane/ether): $\nu_{C{\equiv}C}$ 2188/2169 m/vs, 2033/2036 vs/vs. ^1H NMR (δ, $CDCl_3$): 2.11 (s, ≡CH), 0.21 (s, $Si(CH_3)_3$). $^{13}C\{^1H\}$ NMR (ppm, THF-d_8): 88.7 (s, SiC≡*C*; d, $^3J_{CH}$ = 6.2 Hz without ^1H decoupling [6a]), 83.1 (s, Si*C*≡C; decet, $^3J_{CH}$ = 2.7 Hz [6a]), 69.2 (s, C≡*C*H; d, $^1J_{CH}$ = 258.8 Hz [6a]), 68.9 (s, *C*≡CH; d, $^2J_{CH}$ = 47.9 Hz [6a]), –0.90 (s, $SiCH_3$; qsept, $^1J_{CH}$ = 120.3 Hz, $^3J_{CH}$ = 2.0 Hz).

$Me_3SiC{\equiv}CC{\equiv}CBr$ [14]

Method **A**. A three-neck flask was charged with $Me_3SiC{\equiv}CC{\equiv}CH$ (5.7 g, 47 mmol) [6a, 10] and ether (100 mL) and fitted with a gas inlet, reflux condenser, and dropping funnel. Then EtMgBr (3.0 M in ether, 17 mL, 51 mmol) was added with stirring. The mixture was refluxed. After 1 h, the mixture was cooled to –45 °C and Br_2 (2.9 mL, 8.9 g, 56 mmol) was slowly added. The mixture was allowed to warm to room temperature and poured into water. The aqueous phase was extracted with ether (3 × 50 mL). The combined organic phases were dried over $MgSO_4$. The solvent was removed by rotary evaporation and the residue was vacuum distilled. A pale yellow fraction was collected (45–51 °C, 3 mm Hg) to give spectroscopically pure $Me_3SiC{\equiv}CC{\equiv}CBr$ (2.07 g, 10 mmol, 22%). IR (cm^{-1}, ether): $\nu_{C{\equiv}C}$ 2175 vs, 2095 s. ^1H NMR (δ, C_6D_6): 0.012 (s, CH_3). $^{13}C\{^1H\}$ NMR (ppm, C_6D_6): 89.4 (s, SiC≡*C*), 84.1 (s, Si*C*≡C), 67.0 (s, *C*≡CBr), 41.5 (s, C≡*C*Br), 0.2 (s, $SiCH_3$).

Method **B**. A round-bottom flask was charged with $Me_3SiC{\equiv}CC{\equiv}CH$ (4.920 g, 40.01 mmol), $AgNO_3$ (2.039 g, 12.00 mmol), and acetone (10 mL). The mixture was stirred, and after 20 min, ether (100 mL) and NBS (9.966 g, 56.01 mmol) were added. The disappearance of the starting diyne was monitored by IR. After 12 h, the mixture was filtered and the flask was rinsed with ether (2 × 10 mL). Then ice water (40 mL) was poured onto the combined filtrates with stirring. The aqueous phase was extracted with ether (2 × 20 mL). The combined organic phases were dried over Na_2SO_4. The solvents were removed by rotary evaporation at room temperature and the residue was distilled by oil pump vacuum (43° C, 0.15 mm Hg) to give colorless $Me_3SiC{\equiv}CC{\equiv}CBr$ (4.74 g, 23.6 mmol, 59%) that was stored in a freezer. IR (cm^{-1}, film): $\nu_{C{\equiv}C}$ 2177 vs, 2095 s. ^1H NMR (δ, $CDCl_3$): 0.20 (s, CH_3).

Crystallography

A benzene solution of **8** was layered with hexane. After 8 days, dark red prisms had formed. Data were collected as outlined in Table I. Cell constants were obtained from 25 reflections with $25° < 2\theta < 30°$. The space group was determined from systematic absences ($h0l$: $h + l = 2n$; $0k0$: $k = 2n$) and subsequent least-squares refinement. Lorentz, polarization, and empirical absorption (Ψ scans) corrections were applied. The structure was solved by standard heavy-atom techniques with the Molen/VAX package [33]. Non-hydrogen atoms were refined with anisotropic thermal parameters. The weighting scheme used a non-Poisson contribution. Hydrogen atom positions were calculated and added to the structure factor calculations, but were not refined. Scattering factors, and $\Delta f'$ and $\Delta f''$ values, were taken from the literature [34].

Atomic coordinates have been deposited with the Cambridge Crystallographic Data Centre and can be obtained on request at the CCDC, Union Road, Cambridge CB2 1EZ, UK. Structure factors and thermal parameters have been deposited with the British Library, Document Supply Centre at Boston Spa, Wetherby, West Yorkshire, LS23 7BQ, UK, as supplementary publication No. = SUP 90447 and are available on request from the Document Supply Centre.

Acknowledgement

We thank the NSF for support of this research.

References

[1] (a) Beck W., Niemer B., Wieser M., *Angew. Chem. Int. Ed. Engl.*, 1993, **32**, 923. (b) Lang H., *Angew. Chem. Int. Ed. Engl.*, 1994, **33**, 547. (c) Akita M., Moro-oka Y., *Bull. Chem. Soc. Jpn.*, 1995, **68**, 420. (d) Bunz U., *Angew. Chem. Int. Ed. Engl.*, 1996, **35**, 969.

[2] For the longest metal-capped *sp*-carbon chain compounds prepared in other laboratories to date see: Coat F., Lapinte C., *Organometallics*, 1996, **15**, 477; Bruce M. I., Ke M., Low P. J., *J. Chem. Soc., Chem. Commun.*, 1996, 2405.

[3] (a) Mel'nichenko V. M., Sladkov A. M., Nikulin Yu. N., *Russ. Chem. Rev.*, 1982, **51**, 421. (b) Smith P. P. K., Buseck P. R., *Science*, 1982, **216**, 984. (c) Kasatochkin V. I., Sladkov A. M., Kudryavtsev Y. P., Popov N. M., Korshak V. V., *Dokl. Chem.*, 1967, **177**, 1031. (d) Akagi K., Nishiguchi M., Shirakawa H., Furukawa Y., Harada I., *Synth. Metals*, 1987, **17**, 557.

[4] For important recent advances see: Lagow R. J., Kampa J. J., Wei H.-C., Battle S. L., Genge J. W., Laude D. A., Harper C. J., Bau R., Stevens R. C., Haw J. F., Munson E., *Science*, 1995, **267**, 362.

[5] Preliminary communications: (a) Zhou Y., Seyler J. W., Weng W., Arif A. M., Gladysz J. A., *J. Am. Chem. Soc.*, 1993, **115**, 8509. (b) Seyler J. W., Weng W., Zhou Y., Gladysz J. A., *Organometallics*, 1993, **12**, 3802. (c) Brady M., Weng W., Gladysz J. A., *J. Chem. Soc., Chem. Commun.*, 1994, 2655. (d) Bartik T., Bartik B., Brady M., Dembinski R., Gladysz J. A., *Angew. Chem. Int. Ed. Engl.*, 1996, **35**, 414.

[6] Full papers: (a) Weng W., Bartik T., Brady M., Bartik B., Ramsden J. A., Arif A. M., Gladysz J. A., *J. Am. Chem. Soc.*, 1995, **117**, 11922. (b) Brady M., Weng W., Zhou Y., Seyler J. W., Amoroso A. J., Arif A. M., Böhme M., Frenking G., Gladysz J. A., *J. Am. Chem. Soc.*, 1997, **119**, 775.

[7] Lead reference for compounds with odd carbon chains: Weng W., Bartik T., Gladysz J. A., *Angew. Chem. Int. Ed. Engl.*, 1994, **33**, 2199.

[8] Sonogashira K. In *Comprehensive Organic Synthesis*, Trost B. M., Fleming I., Eds., Pergamon, New York, 1991, Vol. 3, p. 551.

[9] Eglinton G., McCrae W., *Adv. Org. Chem.*, 1963, **4**, 225.

[10] To our knowledge, this exact desilylation/protonation sequence has not been described in the literature. Thus, our procedure is given in the experimental section. However, each step has been previously communicated: (a) Holmes A. B., Jennings-White C. L. D., Schulthess A. H., Akinde B., Walton D. R. M., *J. Chem. Soc., Chem. Commun.*, 1979, 840. (b) Holmes A. B., Jones G. E., *Tetrahedron Lett.*, 1980, **21**, 3111. (c) Zweifel G., Rajagopalan S., *J. Am. Chem. Soc.*, 1985, **107**, 700. (d) Shim S. C., Lee T. S., *Bull. Korean Chem. Soc.*, 1986, **7**, 357.

[11] (a) Eastmond R., Johnson T. R., Walton D. R. M., *Tetrahedron*, 1972, **28**, 4601. (b) Yamaguchi M., Park H.-J., Hirama M., Torisu K., Nakamura S., Minami T., Nishihara H., Hiraoka T., *Bull. Chem. Soc. Jpn.*, 1994, **67**, 1717.

[12] Walton D. R. M., Waugh F., *J. Organomet. Chem.*, 1972, **37**, 45.

[13] (a) Cadiot P., Chodkiewicz W. In *Chemistry of Acetylenes*, Viehe H. G., Ed., Marcel Dekker, New York, 1969, p. 614. (b) For recent literature, see the following articles and references therein: Alami M., Ferri F., *Tetrahedron Lett.*, 1996, **37**, 2763; Barbu E., Tsibouklis J., *Tetrahedron Lett.*, 1996, **37**, 5023.

[14] de Graaf W., Smits A., Boersma J., van Koten G., Hoekstra W. P. M., *Tetrahedron*, 1988, **44**, 6699.

[15] Eastmond R., Walton D. R. M., *Tetrahedron*, 1972, **28**, 4591.

[16] (a) Hofmeister H., Annen K., Laurent H., Wiechert R., *Angew. Chem. Int. Ed. Engl.*, 1984, **23**, 727. (b) Nishikawa T., Shibuya S., Hosokawa S., Isobe M., *Synlett*, 1994, 485.

[17] Rubin Y., Lin S. S., Knobler C. B., Anthony J., Boldi A. M., Diederich F., *J. Am. Chem. Soc.*, 1991, **113**, 6943.

[18] The closest analogies of which we are aware involve the μ^3 bromocarbyne complex $BrCCo_3(CO)_9$, and organic terminal alkynes, as opposed to two alkyne coupling partners: (a) Worth G. H., Robinson B. H., Simpson J., *Organometallics*, 1992, **11**, 501. (b) Worth G. H., Robinson B. H., Simpson J., *J. Organomet. Chem.*, 1990, **387**, 337.

[19] Torkington P., *Proc. Roy. Soc.*, 1951, **A206**, 17.

[20] March J., *Advanced Organic Chemistry*, 4th ed., Wiley, New York, 1992, 21-22.

[21] (a) Nitta I., *Acta Crystallogr.*, 1960, **13**, 1035. To our knowledge, the atomic coordinates for diphenyl 1,3,5,7-octatetrayne are not in the Cambridge Crystallographic Data Base or otherwise available. (b) For additional data see: Watanabé T., Taguchi I., Masaki N., *Acta Crystallogr.*, 1959, **12**, 347.

[22] Coles B. F., Hitchcock P. B., Walton D. R. M., *J. Chem. Soc., Dalton Trans.*, 1975, 442.

[23] Altmann M., Enkelmann V., Bunz U. H. F., *Chem. Ber.*, 1996, **129**, 269.

[24] (a) Kiel W. A., Lin G.-Y., Constable A. G., McCormick F. B., Strouse C. E., Eisenstein O., Gladysz J. A., *J. Am. Chem. Soc.*, 1982, **104**, 4865. (b) Peng T.-S., Arif A. M., Gladysz J. A., *J. Chem. Soc., Dalton Trans.*, 1995, 1857. (c) It would be more instructive to compare the conformation of **8** with that of a complex of **I** (or the cyclopentadienyl analog) and a tricoordinate donor atom in which all substituents are identical (e.g., XR_3). However, no such species have been structurally characterized to date.

[25] Goddard R., Haenel M. W., Herndon W. C., Krüger C., Zander M., *J. Am. Chem. Soc.*, 1995, **117**, 30, and references therein.

[26] For an analysis of the packing of crystalline 1,3,5-triynes see: Enkelmann V., *Chem. Mat.*, 1994, **6**, 1337.

[27] In the same vein, with the smaller phenyl, *t*-butyl, and trimethylsilyl endgroups, the longest dimension of the unit cell is nearly twice as great as the intermediate dimension. However, with the larger cobalt- and rhenium-containing endgroups, the two longest unit cell dimensions are much more comparable.

[28] *Modern Acetylene Chemistry*, Stang P. J., Diederich F., Ed., VCH, New York, 1995.

[29] (a) Juaristi E., Cruz J. S., Martinez- Richa A. In *Abstracts of Papers*, 181st National Meeting of the Americal Chemical Society, Atlanta, Georgia, March 1981, American Chemical Society: Washington, D.C., 1981, ORGN 236. (b) See also *Aldrichimica Acta*, 1981, **14**, 59.

[30] Kofron W. G., Baclawski L. M., *J. Org. Chem.*, 1976, **41**, 1879.

[31] The yield obtained in this procedure, which is still being optimized, is a function of the silica gel employed. IR monitoring is beneficial, and alternative workups will be described in a future publication.

[32] The $\equiv C$ ^{13}C NMR assignments were made on the basis of trends described earlier ($^2J_{CP} > {}^4J_{CP} > {}^3J_{CP}$, $^5J_{CP}$) [6a]. Also, $C\equiv CSi$ resonances are normally downfield of internal $C\equiv C$ resonances due to well established anisotropy effects [5d].

[33] Frenz B. A., "The Enraf-Nonius CAD4 SDP–A Real-time System for Concurrent X-ray Data Collection and Crystal Structure Determination". In *Computing and Crystallography*, Schenk H., Olthof-Hazelkamp R., van Konigsveld H., Bassi G. C., Eds., Delft University, Delft, Holland, 1978, 64-71.

[34] Cromer D. T., Waber J. T. In *International Tables for X-ray Crystallography*, Ibers J. A., Hamilton W. C., Eds., Kynoch, Birmingham, England, 1974, Vol. IV, 72-98, 149-150, Tables 2.2B and 2.3.1.

[35] Anisotropically refined atoms are given in the form of the isotropic equivalent displacement parameter defined as: $(4/3)[a^2B(1,1)+b^2\ B(2,2)+c^2B(3,3)+ab(\cos\gamma)B(1,2)+ac(\cos\beta)B(1,3)+bc\ (\cos\beta)B(2,3)]$.

[36] The form of the anisotropic displacement parameter is: $\exp[-2\pi^2\{h^2a^2U(1,1) + k^2b^2U(2,2) + l^2c^2U(3,3) + 2hkabU(1,2) + 2hlacU(1,3) + 2klbcU(2,3)\}]$ where a, b, and c are reciprocal lattice constants.